International Research Journal of Engineering and Technology (IRJET) e-ISSN: 2395-0056
Volume: 08 Issue: 06 | June 2021 www.irjet.net p-ISSN: 2395-0072

Design and Simulation of a Fluid-filled D-Shaped Lens for Solar Thermal Applications

Naleli Jubert Matjelo[1], Thaane Emmanuel Mokose[1], Molibeli Rakauoane[1]

[1]*National University of Lesotho, Department of Physics and Electronics, P. O. Roma 180, Lesotho*

Abstract - *In this article, we derive an analytical model for a fluid-filled D-shaped lens based on Snell's law. The general approach taken here is to combine Snell's law with geometric analysis to derive a differential equation describing how the lens surface should be curved to converge parallel light rays onto one focal point. This derived differential equation yields four solutions; two of which are extraneous (hence thrown away), while the other two are physically realizable and therefore used as lens models in the simulation. The lens models are intended for solar thermal heating, especially in rural areas where means of cooking and water heating are limited.*

***Key Words*: Snell's law, D-shaped lens, Solar Thermal, Chromatic Aberrations, Differential Equation, Extraneous Solution, Converging Rays.**

1. INTRODUCTION

Lensing is one of the most widely occurring optical phenomena not just on earth but in the universe at large. Snell's law [1] is at the roots of most of these lensing phenomena including rainbow, halo, and corona. A lens is used in many applications including optical telescopy [2] and optometry, spectroscopy and microscopy [3], mobile cameras, and solar thermal applications [4], [5]. The traditional design of a lens is a numerical and forward process based on raytracing and aberration theory [6], [7]. Some of the design methods rely on numerical optimization for automation [8]. In [9] a three-dimensional analytical derivation for a lens surface is presented and it is shown that it leads to a partial differential equation. In [10] a method for calculating the meridian profile of the aspherical surface (i.e. paraboloids, ellipsoids, hyperboloids, oblate spheroids, etc obtained by rotating conical sections) of a plane-convex lens that exclude spherical aberration is proposed. The resulting differential equation could only be solved numerically, however. In this paper, we formulate the problem of a D-shaped lens surface shape directly from geometrical analysis constrained by Snell's law in two dimensions. The derived ordinary differential equation is solved analytically and solutions are generalized to three dimensions. Solar thermal application models are proposed and simulated based on the two solutions obtained from the derivation.

One lens application that motivated the work in this paper is that of solar thermal concentrator for cooking and water heating [4], [5], [11], [12] as part of making use of renewable energy from the sun. The means of cooking, water heating, and housewarming in developing countries are very limited and even those that are available are quite challenging to obtain [13]. The use of solar thermal as a means for cooking and heating, in general, is not yet widely adopted in the rural areas of Lesotho [13]. Despite that being the case, solar cooking is arguably one of the best options that can be used to relieve the pressure of all-time fuel requirements in rural areas [14], [15]. As an example, one would have to gather wood every day to carry daily operations such as cooking, water heating, and house warming [13].

The rest of this paper is structured as follows. Section II gives a detailed account of the formulation of a D-shaped lens surface structure. This includes deriving the ordinary differential equation governing the refraction of incident light rays to a single point at the focus. The differential equation is solved analytically and the solutions generalized to three dimensions. Section III builds upon the solutions from the previous section, which are used to guide the design process including parameter identification. The proposed D-shaped lens design is a hollow shell to be filled with an appropriate fluid to operate as a solar thermal concentrator. Section IV concludes this paper by outlining the major aspects of this work.

2. MODEL FORMULATION

A converging lens problem can be posed as the problem of finding an equation for a surface of a transparent material, such that parallel light rays hitting this material at some orientation results in all light rays being refracted and converging at a single point called the focal point. One way of addressing this problem is by using Snell's law on some arbitrary surface and enforce a constraint of concurrency on all refracted light rays. This is the approach adopted in this work.

2.1 Geometric Analysis

Consider a curve $z(x)$ in 2D which is supposed to refract every line incident on it such that the refracted lines are all concurrent as shown in Fig. 1 below. The parameters m_1, m_2, m_3 and m_4 are slopes for incident light ray, refracted light ray, tangent line, and normal line respectively. Parameters θ_i and θ_t represent angles of incidence and transmission respectively and their respective complementary angles as ϕ_i and ϕ_t.

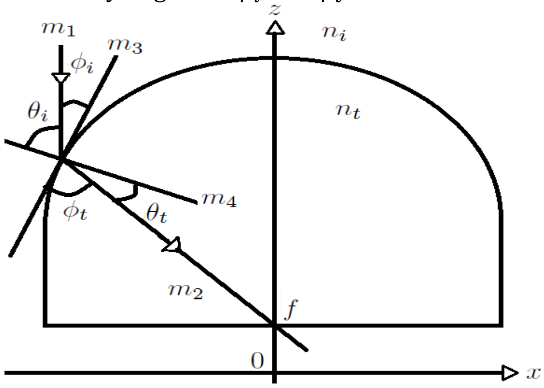

Fig. 1: Converging D-shaped lens schematic.

The refractive indices n_i and n_t are dielectric properties of incidence and transmission media respectively. The focal point and the turning point of the lens are denoted by parameters f and c respectively. The transmission of light rays from incidence medium to transmission medium is governed by Snell's law as indicated below,

$$n_i \cos(\phi_i) = n_t \cos(\phi_t) \tag{1}$$

It can be inferred from Fig. 1 that the slopes are given by the following equations,

$$m_1 = \infty \tag{2}$$

$$m_2 = (z - f)x^{-1} \tag{3}$$

$$m_3 = \dot{z} \tag{4}$$

$$m_4 = -\dot{z}^{-1} \tag{5}$$

with $\dot{z} = dz/dx$. From the equations (2 - 5) above, it can be shown that the terms $\cos^2(\phi_i)$ and $\cos^2(\phi_t)$ can be represented as follows,

$$\cos^2(\phi_i) = \frac{\dot{z}^2}{1+\dot{z}^2} \tag{6}$$

$$\cos^2(\phi_t) = \frac{(x+(z-f)\dot{z})^2}{(x+(z-f)\dot{z})^2+(z-f-x\dot{z})^2} \tag{7}$$

Substituting equations (6 - 7) into equation (1) and rearranging terms we obtain the following differential equation,

$$(n^2-1)[(z-f)^2+x^2]\dot{z}^4 + 2n^2(z-f)x\dot{z}^3 + (n^2-1)[(z-f)^2+x^2]\dot{z}^2 + 2n^2x(z-f)\dot{z} - n^2x^2(\dot{z}^4-1) = 0 \tag{8}$$

with $n = n_t/n_i$ as the relative refractive index.

2.2 Reduced Differential Equation

The differential equation (8) above can be factored into the following equations,

$$\dot{z}^2 + 1 = 0 \tag{9}$$

$$\dot{z}^2 = \frac{-2n^2(z-f)x\dot{z}+n^2(\dot{z}^2-1)x^2}{(n^2-1)(z-f)^2+x^2} \tag{10}$$

Equation (9) gives rise to our first two extraneous solutions, $z = \pm ix + c$ for some integration constant c and imaginary number $i = (-1)^{\frac{1}{2}}$. Equation (10) can be factored further until it yields the equations,

$$\dot{z} = \frac{\pm nx}{\sqrt{x^2+(z-f)^2} \mp n(z-f)} \tag{11}$$

The analysis carried out above is for a case whereby the focal point is aimed to be inside the curved surface, thus the light rays are incident on the curved surface. In Fig. 2 below, we have a different situation in which the light is incident on the flat part and exit on the curved part of the D-shaped lens.

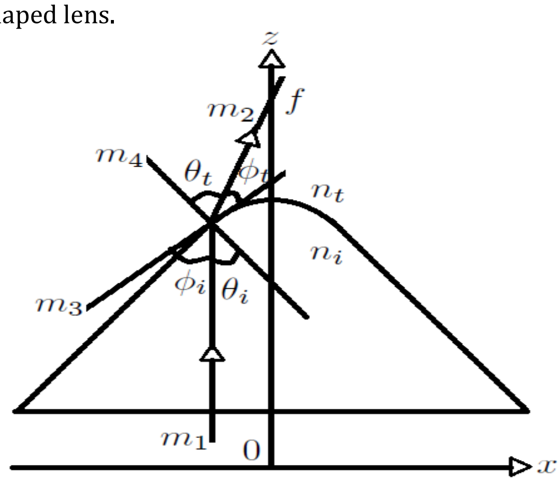

Fig. 2: Alternative setup for a D-shaped lens.

Interestingly, it can be shown, through the analysis as done above, that in this case, the solution has the same structure as the one we obtained in equation (11) above, with the only exception that the relative refractive index n in equation (11) is now replaced by its reciprocal to give the following solution,

$$\dot{z} = \frac{\pm nx}{n\sqrt{x^2+(z-f)^2} \mp (z-f)} \tag{12}$$

The solutions to these two first-order nonlinear differential equations (11 - 12) are presented in the next section.

2.3 2D Solutions and Model Selection

Solving the two nonlinear first-order differential equations (11 - 12) we obtain the following solutions respectively,

$$z(x) = \frac{n(c+nf) \pm n\sqrt{(nc+f)^2+(1-n^2)x^2}}{n^2-1} \tag{13}$$

$$z(x) = \frac{(nc+f) \pm \sqrt{(nf+c)^2+(n^2-1)x^2}}{n^2-1} \tag{14}$$

with equation (13) being the solutions corresponding to the lens model with a focal point inside the curved surface while equation (14) is for the lens model with the focal point outside the curved surface. Two of the four solutions in equations (13 - 14) are extraneous solutions that do not satisfy Snell's law but rather satisfy the relation, $n_i \cos(\phi_i) = -n_t \cos(\phi_t)$. The first extraneous solution is given by,

$$z(x) = \frac{n(c+nf) - n\sqrt{(nc+f)^2 + (1-n^2)x^2}}{n^2-1} \quad (15)$$

and its simulation is shown in Fig. 3 below,

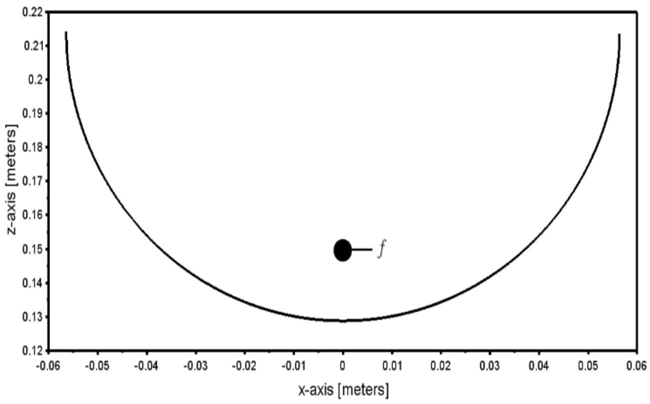

Fig. 3: In-focusing extraneous solution.

It can be seen from Fig. 3 above that any vertically oriented rays incident on the curved line cannot all be concurrent at the labeled focal point $(0, f)$. It can be shown with manual ray-tracing of few points that this solution does not satisfy Snell's law (i.e. $n_i \cos(\phi_i) = n_t \cos(\phi_t)$) but rather satisfies an almost similar relation, (i.e. $n_i \cos(\phi_i) = -n_t \cos(\phi_t)$). The second extraneous solution, suffering the same fate, is the one described as follows,

$$z(x) = \frac{(nc+f) + \sqrt{(nf+c)^2 + (n^2-1)x^2}}{n^2-1} \quad (16)$$

which is simulated in Fig. 4 below.

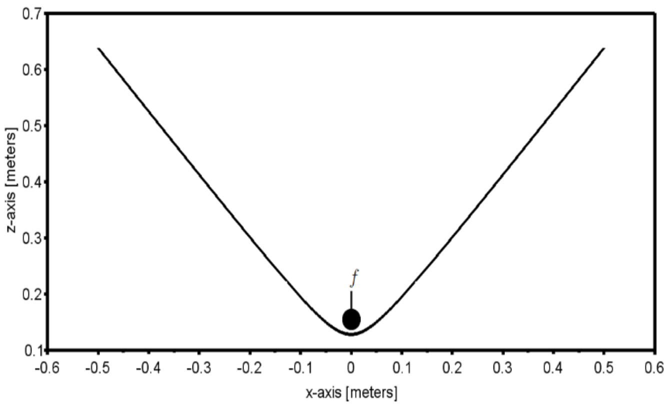

Fig. 4: Out-focusing extraneous solution.

The focal point for this solution is also located at the point where it becomes impossible for any vertically oriented rays to refract on the curve and be all concurrent on that focal point. Now that we have identified and put aside the extraneous solutions (i.e. equations (15 - 16), the next section will elaborate more on the solutions satisfying Snell's law.

2.4 Model Analysis & 3D Generalization

2.4.1 Model One

This model from equation (13), with an internal focal point, has a turning point at $(0, \frac{n(f+c)}{n^2-1})$ and curvature of $\ddot{z} = -\frac{n}{f+nc}$. Since c is an arbitrary integration constant, we can choose it to take any value in design. Here we choose it as $c = (n-2)f/n$ such that the distance from the turning point to $(0, f)$ is exactly equal to the focal length f itself. With that choice, the turning point becomes $(0, 2f)$ and the curvature becomes $\ddot{z} = \frac{-n}{(n-1)f} < 0$, thus the turning point is a maximum. It can also be shown that the model is real only for the values of x in the interval,

$$x \in \left[-f\sqrt{\frac{n-1}{n+1}}, f\sqrt{\frac{n-1}{n+1}}\right] \quad (17)$$

Beyond this interval, the model gives complex values, thus physically unrealistic. This model can conveniently be used as an automated solar thermal kettle since it is in-focusing. That is, an absorbing element is placed at the focal point and water (with $n \approx 1.33$) used to fill the lens. The refracted rays converge onto the element and heat it, which in turn heats the water around it. At the point when water starts boiling, the bubbles formed start dispersing light rays such that convergence to the focal point is compromised. This means water will start to cool down until bubbles disappear, at which point the element starts to heat the water again. This behaviour bears much resemblance to how a thermostat works in automated devices and appliances. The final model equation is given as,

$$z(x) = \frac{n+2}{n+1}f + \frac{n}{n+1}\sqrt{f^2 - \frac{n+1}{n-1}x^2} \quad (18)$$

which is simulated in Fig. 5 below. It can be confirmed with manual ray-tracing of few points that the rays incident on the curved surface from above will indeed refract and all be concurrent at the focal point $(0, f)$. This 2D version can be used for making a cylindrical D-shaped lens that focuses light rays inwards towards a focal line rather than a focal point.

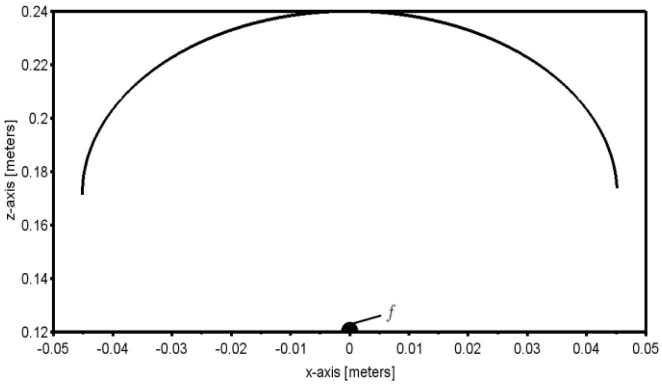

Fig. 5: In-focusing acceptable solution.

The three-dimensional generalization of this solution can be made by rotating the two-dimensional solution about the z −axis to obtain the following solution,

$$z(x,y) = \frac{n+2}{n+1}f + \frac{n}{n+1}\sqrt{f^2 - \frac{n+1}{n-1}(x^2+y^2)} \quad (19)$$

and its simulation is shown in Fig. 6 below. This 3D solution model is appropriate for designing domeshaped D-shaped lenses rather than cylindrical D-shaped lenses.

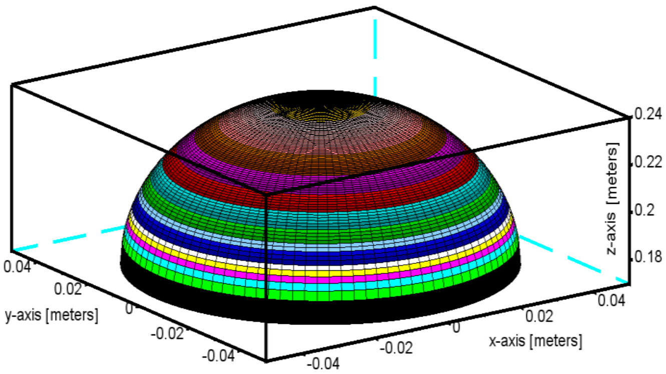

Fig. 6: In-focusing acceptable solution generalized to 3D.

2.4.2 Model Two

This model from equation (14), with an outside focal point, has a turning point at $(0, \frac{f+c}{1-n})$ and curvature of $\ddot{z} = -\frac{n}{f+nc}$. Since c is an arbitrary integration constant, we can choose it to take any value in design. Here we choose it as $c = -f$ such that the distance from the turning point to $(0, f)$ is exactly equal to the focal length f itself. With that choice, the turning point becomes $(0,0)$ and the curvature becomes $\ddot{z} = \frac{-n}{nf} < 0$, thus the turning point is a maximum. In this, the allowed values of x are in the interval,

$$x \in (-\infty, +\infty) \quad (20)$$

This model works like a common D-shaped lens and can be used for magnification and solar thermal applications. The final model equation can be written as,

$$z(x) = \frac{1}{n+1}f + \frac{1}{n+1}\sqrt{f^2 + \frac{n+1}{n-1}x^2} \quad (21)$$

with its simulation shown in Fig. 7 below.

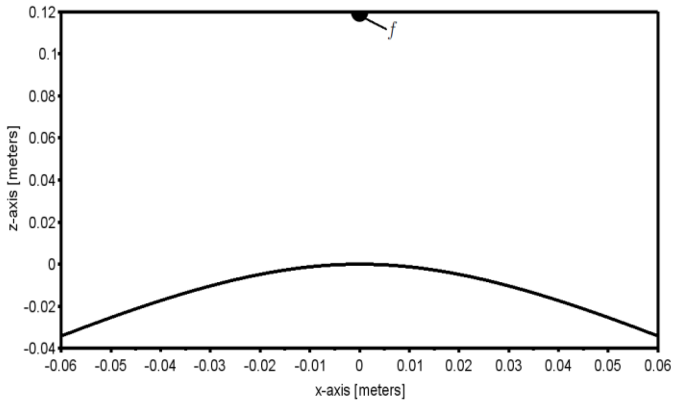

Fig. 7: Out-focusing acceptable solution in 2D.

This 2D version can be used for making a cylindrical D-shaped lens that focuses light rays outwards towards a focal line rather than a focal point. The extension to three dimensions can be done by rotating the two-dimensional solution about the z −axis to obtain the equations,

$$z(x,y) = \frac{1}{n+1}f + \frac{1}{n+1}\sqrt{f^2 + \frac{n+1}{n-1}(x^2+y^2)} \quad (22)$$

which is also shown as a simulation in Fig. 8 below.

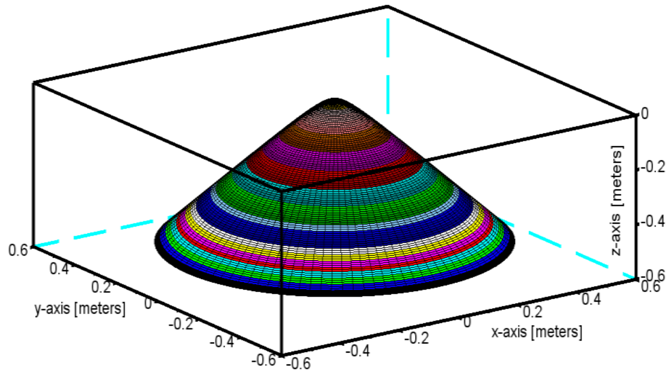

Fig. 8: Out-focusing acceptable solution in 3D.

This solution is more useful for design involving dome-shaped lenses rather than cylindrical ones. The design parameters for prototypes, as well as some simulations, are shown in the next section.

3. DESIGN AND PROPOSED IMPLEMENTATION

3.1 Cylindrical In-Focusing Solar Kettle

Here we use the model in equation (18) to design the prototype for a cylindrical solar kettle. Fig. 9 below shows the design structure.

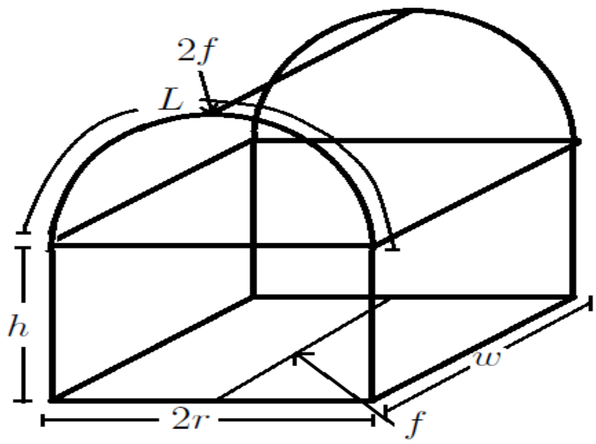

Fig. 9: Schematic of an automated cylindrical solar kettle.

The design parameters are listed below,
1) Relative refractive index, $n = 1.33$.
2) Focal point, $(x, f) = (0.00m, 0.12m)$.
3) Turning point $(x, z) = (0.00m, 0.24m)$.
4) Reservoir box dimensions, $2r \times w \times h = 0.09m \times 0.09m \times 0.06m$.
5) From equation (18), the length of the curved sheet is, $L = \int_{-0.045m}^{+0.045m} \sqrt{1 + \dot{z}^2} dx \approx 0.17m$.

Only the curved surface needs to be made of transparent material. For large rigid structures, we recommend a polycarbonate sheet with a refractive index ranging from 1.57 to 1.61 in the visible range. The sheet is slightly flexible to bend but maintains some rigidity in its structure even after bending. The rest of the bottom reservoir box can be made of any rigid material, even if not transparent. For a simple prototype like the one described here, one can use recycled pieces of hard plastic parts that can be glued and sealed together to make a complete structure. The semi-curved sidewalls should be made of rigid material (opaque or transparent) to give shape and structure to the curved transparent roof surface.

The bottom surface can be made darker for better absorption of heat from the refracted rays. The hemispherical design, from equation (19), would follow pretty much the same procedure and design parameters with the exception that the reservoir will now be round/cylindrical instead of being rectangular, and also the curved refracting surface will no longer be cylindrical but rather hemispherical or dome-shaped. The implementation of this variation involves cutting out some slices and merging others (with glue) to give a dome of the right shape. This is not as simple as in the previous cylindrical design.

3.2 Cylindrical Out-Focusing Heat Concentrator

Here we use the model equation (21) to design the prototype for a cylindrical solar concentrator. Fig. 10 below shows the design structure.

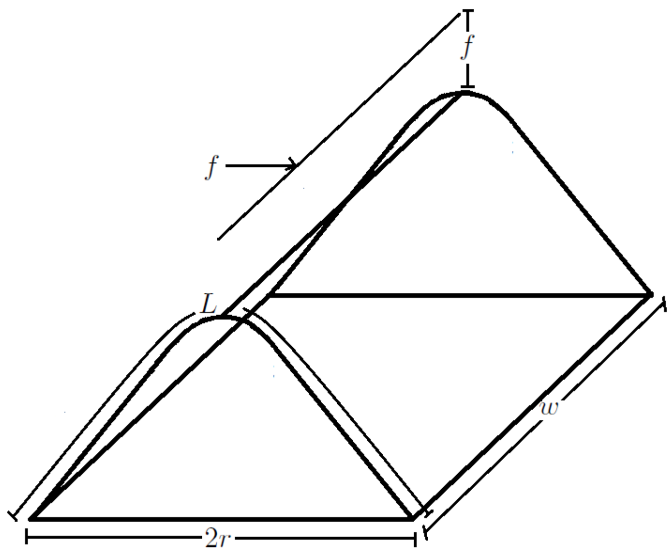

Fig. 10: Schematic of out-focusing heat concentrator.

The design parameters are listed below,

1) Relative refractive index, $n = 1{:}33$.
2) Focal point, $(x, f) = (0.00m, 0.12m)$.
3) Turning point $(x, z) = (0.00m, 0.00m)$.
4) Reservoir box dimensions, $2r \times w \times h = 0.12m \times 0.12m \times 0.035m$.
5) From equation (21), the length of the curved sheet is, $L = \int_{-0.06m}^{+0.06m} \sqrt{1 + \dot{z}^2} dx \approx 0.141m$.

Here all surfaces should be made of transparent material except for the two side pieces, which can be made of either transparent or opaque but rigid material. For large structures, we recommend polycarbonate sheets for the parts requiring transparent material. Similar to the case in the previous section, the hemispherical design, which follows equation (22), would follow pretty much the same procedure and design parameters with the exception that the reservoir will now be round/cylindrical instead of being rectangular and also the curved refracting surface will no longer be cylindrical but rather hemispherical or dome-shaped. As can be inferred from the material used to build the prototypes, the cost of producing these designs is relatively low compared to glass/perspex-based lenses. As an example here is the list of projected costs in producing the two prototypes,

1. The opaque parts recycled at zero cost, $M0.00$.
2. Water costs nothing, $M0.00$.
3. The polycarbonate sheet costs $M600.00$ per square meter, hence only $M32.00$ would be spent on sheets for both prototypes.
4. Glue for bonding costs $M50.00$.

These lens designs can be made big and yet remains lighter for transportation since the fluid can be pumped out during transportation. The refracting material used for larger designs has to take into account the geometrical deformations introduced by fluid weight and heat. This means parameters like flexibility, thickness, and rigidity of the sheet and structure as a whole need to be carefully looked into.

In the case whereby the refractive indices of the fluid and the transparent sheet differ significantly, the thickness of the sheet would influence the convergence of light rays (to the focus) significantly. This adds to the chromatic aberrations problem which leads to the light of different frequencies focusing at different focal points. One can suggest the following quick solutions,

- Replacing polycarbonate sheet with some other transparent material whose refractive index (in the visible regime) is close to that of the fluid inside.
- Replacing the fluid with the fluid having a refractive index close to that of a polycarbonate sheet.
- Adding impurities, like salts, to the existing fluid until its refractive index comes close to that of the polycarbonate sheet.

3. CONCLUSIONS

In this paper, we have carried out the formulation of a D-shaped lens problem, whose solutions led to two possible designs of D-shaped lens; in-focusing and out-focusing lenses. The design process was carried out based on these two solutions and resulted in two fluid-filled D-shaped lens models whose prototypes were proposed. It was anticipated that the thickness (combined with a refractive index different from that of fluid) of the polycarbonate sheet would result in a significant deviation of refracted rays from the focal point/line. Possible solutions suggested were (i) replacing polycarbonate sheet with some other transparent material whose refractive index (in the visible regime) is close to that of the fluid inside or (ii) replacing the fluid with the fluid having a refractive index close to that of polycarbonate sheet or (iii) adding impurities like salts to the existing fluid until its refractive index comes close to that of the polycarbonate sheet. The cost of producing these designs was found to be relatively low compared to glass/perspex-based lenses and also these lens designs are lighter since the fluid can be pumped out during transportation. We maintain that these cheap lens designs can be of great help in complementing the fuel-based (and other solar thermal-based) means of heating and cooking in developing countries like Lesotho, especially in rural areas.

REFERENCES

[1] J. Griffiths David. Introduction To Electrodynamics. Pearson Education Inc, 4th edition, 2013.
[2] G. Oesper D. Bimey, D. S. Gonzalez. Observational Astronomy. University Press, Cambridge, 2006.
[3] D. A. Peterson. Confocal Microscopy. Encyclopedia of Movement Disorder, 2010.
[4] S. Zhao W. Qandil, H. Wang. Application-based design of the Fresnel lens solar concentrator. Renewables, 6(3), 2019.
[5] R. Suzuki A. Leutz. Nonimaging Fresnel Lenses, chapter Lenses, and Mirrors for Solar Energy, page 3. Springer, Berlin, Heidelberg, 2001.
[6] Z. Malacara-Hernandez, D. Malacara-Hernandez. Handbook of Optical Design: Chapter 13. CRC Press, second edition (optical engineering) edition, 2003.
[7] C. Kweon, G. Kim. Aspherical Lens Design by Using a Numerical Analysis. Journal of the Korean Physical Society, 51(1), July 2007.
[8] W. J. Smith. Modern Optical Engineering: The Design of Optical Systems - Page 431. New York: McGraw-Hill Professional, third edition, 2000.
[9] L. Yang, L. Vasudevan. An inverse and analytic lens design method. arXiv:1603.05306 [physics.optics], 2016.
[10] I. Evteev. Differential equation of an aspherical lens and its solution. arXiv:1705.01155 [astro-ph], 2017.
[11] C. K. Cheng, T. C. Yang. Biaxial-Type Concentrated Solar Tracking System with a Fresnel Lens for Solar-Thermal Applications. Appl. Sci., 6(4):115, 2016.
[12] N. B. Lionel Beneston S. Berin Aniesh. Review on the Applications of Fresnel Lens in Solar Radiation Concentrator. International Journal of Innovative Research In Science, Engineering and Technology, 6(45941), 2017.
[13] Mothala M. Determinants of choice of household energy use in Lesotho. Master's thesis, National University of Lesotho: Energy Research Centre, May 2020.
[14] J. M. Wilson, M. Green. The feasibility of introducing solar ovens to rural women in Maphephethe. Tydskrif vir Gesinsekologie en Verbruikerswetenskappe, 28:54, 2000.
[15] A. Balghouthi M. Riahi, A. Guizani. Investigation of solar cooker applications for rural and remote areas. Journal of Materials and Environmental Science, 9(8):2438, August 2018.